Draft version February 18, 2025
Typeset using LaTeX default style in AASTeX631

Observation-Based Iterative Map for Solar Cycles. II. The Gnevyshev-Ohl Rule and its Generation Mechanism

Zi-Fan Wang,[1] Jie Jiang,[2,3] and Jing-Xiu Wang[4,1]

[1] *Key Laboratory of Solar Activity, National Astronomical Observatories, Chinese Academy of Sciences, Beijing 100101, China*
[2] *School of Space and Earth Sciences, Beihang University, Beijing, China*
[3] *Key Laboratory of Space Environment Monitoring and Information Processing of MIIT, Beijing, China*
[4] *School of Astronomy and Space Science, University of Chinese Academy of Sciences, Beijing, China*

ABSTRACT

The Gnevyshev-Ohl (G-O) rule, also known as the even-odd effect, is an important observational phenomenon in solar cycles, suggesting that cycles with even indices tend to be followed by stronger cycles. The rule is considered to be related to the solar dynamo, which drives the evolution of the Sun's large-scale magnetic field. However, observational studies of the G-O rule have revealed inconsistencies, particularly regarding long-term variations and the underlying physical mechanisms. In this study, we use an iterative map derived within the framework of the Babcock-Leighton (BL) dynamo to analyze the G-O rule. We investigate comprehensive and definitive forms of the G-O rule using both a sufficiently large number of solar cycles and a limited number of solar cycles. Our findings indicate a higher probability for an arbitrary cycle to be followed by a stronger cycle instead of weaker, regardless of even or odd. Over time spans comparable to historical observations, cycles exhibit periods that follow both the G-O rule and the reversed G-O rule, without a statistically significant preference, consistent with the observed variability of the G-O rule. The occurrence of the reversed G-O rule is random, rather than periodic. The G-O rule emerges as a result of the nonlinearity and stochasticity inherent in the BL mechanism. These results advance our understanding of the solar cycle and pave the way for improved solar dynamo modeling.

1. INTRODUCTION

Since the discovery of the magnetism in sunspots and its alternating sign across adjacent 11-year solar activity cycles by Hale et al. (1919), the 22-year Hale cycle has been one of the most important topic in solar physics. A critical observation phenomenon associated with the Hale cycle is the Gnevyshev-Ohl (G-O) rule, also known as the even-odd effect. As originally identified by Gnevyshev & Ohl (1948), when solar cycles are paired by index, the following odd cycle is stronger than the previous even cycle, a pattern observed for all cycle pairs starting from the 18th century, with the exception of cycles 4 and 5. Hereafter we refer to this as the cycle strength definition of the G-O rule. Gnevyshev & Ohl (1948) also found that the correlation between even cycles and their following odd ones is significantly higher than that between even cycles and their preceding odd cycles, which we will hereafter referred to as the correlation definition of the G-O rule. The G-O rule seemingly shows that the Hale cycle is a fundamental component of the evolution of solar cycles, and raise the important question about its physical origin.

With advancements in observational data and analytical methods, interpretations of the Gnevyshev-Ohl (G-O) rule have diverged in both methodology and results. One key factor contributing to these discrepancies is the different representations of cycle strength. It can be represented either by the total sunspot number, as originally defined by Gnevyshev & Ohl (1948), or by the maximum sunspot number, i.e., the cycle amplitude (e.g. Charbonneau 2005; Javaraiah 2012). The latter representation leads to more violations of the G-O rule (Hathaway 2015), and reduces the statistical significance of the correlation definition (Nagovitsyn et al. 2024). Another point of divergence concerns whether solar cycles should be paired starting with an even or odd cycle. Turner (1925) proposed that cycles should

Corresponding author: Jie Jiang
jiejiang@buaa.edu.cn

be paired starting with the stronger odd cycle, whereas Zolotova & Ponyavin (2015) argued that combination of solar cycles in pairs according to their numbers lacks a physical basis and is not justified. The temporal range over which the G-O rule holds is also debated. Mursula et al. (2001) showed that the G-O rule is in reversed phase between the Maunder and Dalton minima in the cycle strength definition. Usoskin et al. (2001) and Usoskin et al. (2009) suggested that a lost cycle in late 18th century caused the reversal of the G-O rule, while Tlatov (2013) suggests that the G-O rule might be characterized by periodicity reversals. On longer time scales, the validity of the G-O rule remains uncertain. Similä & Usoskin (2023) found no strong statistical evidence for the G-O rule in a millennium-long solar cycle series reconstructed from cosmogenic radioisotopes, possibly due to the significant uncertainty in the reconstructed cycles as explained by the authors. Thus, a comprehensive and definitive description of the G-O rule's form and validity remains elusive.

The physical origin of the G-O rule is closely related to the origin of the solar magnetic field. The formation and evolution of solar large-scale magnetic field are explained by solar global dynamo theories, in which the large-scale field arises from mutually generating poloidal and toroidal fields (Parker 1955; Charbonneau 2020). Early explanations for the origin of the G-O rule often attributed it to the interaction between a non-alternating fossil field and the alternating dynamo field (Mursula et al. 2001). However, Charbonneau et al. (2005) argued that as there are possibly reversals of the G-O rule, fossil field explanation is not favored. Instead, they proposed that the G-O rule can be present in a nonlinear and stochastic dynamo process, independent of fossil fields. In framework of the solar Babcock-Leighton (B-L) type dynamo models (Babcock 1961; Leighton 1969), the generation of toroidal field from poloidal field represented by the polar field at cycle minimum is generally linear (Schatten et al. 1978; Ohl & Ohl 1979; Jiang et al. 2007), while the generation of poloidal field from toroidal field is intrinsically nonlinear and also stochastic (Jiang et al. 2013; Jiang 2020; Karak 2020). Charbonneau et al. (2005) demonstrated that the nonlinear and stochastic mechanisms introduced in a B-L dynamo can generate a G-O rule consistent with the cycle strength definition. Tlatov (2013) conducted simulations with an $\alpha\Omega$ dynamo including nonlinearity and stochastic effects, and found that it also generates properties consistent with the G-O rule. Despite these advancements, the varying interpretations of the G-O rule's form cause ongoing debate on its origin.

When analyzing the dynamo origin of the G-O rule, it is efficient and physically accurate to reduce the dynamo equations into an iterative map of solar cycle strength (May 1976), as long as the properties of the dynamo are well quantified. Durney (2000); Charbonneau (2001); Charbonneau et al. (2005) pioneered the use of iterative maps for solar cycle analysis and applied them to study the G-O rule and other properties of solar cycles. With recent advancements in solar B-L dynamo research, the iterative map can be revisited and applied to analyze and understand the G-O rule.

In the first article of the series, we have constructed an iterative map for solar cycles based on observed nonlinearity and stochasticity in the B-L dynamo. We propose that stochasticity is the primary source of cycle variability and demonstrate how nonlinearity and stochasticity affect the distribution of cycle amplitude. In this sequel, we focus on the G-O rule within the iterative map. We give a comprehensive and definitive description of the G-O rule's form and investigate whether and why the G-O rule emerges as a result of nonlinearity and stochasticity. The results provide implications for theoretical and observational studies on solar dynamo and cycle prediction.

The article is organized as follows. In Section 2 we review the iterative map that we use to analyze the G-O rule. In Section 3 we examine the quantified results of the G-O rule in the iterative map. In Section 4 we explain the nature of the G-O rule. We discuss and conclude in Section 5.

2. REVIEWING THE OBSERVATION BASED ITERATIVE MAP OF SOLAR CYCLES

The B-L dynamo implies a iterative map of cycle strength, in which the strength of a cycle is determined by the strength of its previous cycle. We have produced an observational based iterative map in the prequel to this article, and we review the important points of it briefly here.

Durney (2000) and Charbonneau (2001) first constructed iterative maps of solar cycles by quantifying the mutual generation of poloidal and toroidal field in B-L dynamo. The poloidal field at the beginning of a cycle can be represented by the strength of polar field as well as the global axial dipole field. The poloidal field generates the toroidal field by Ω-effect, which is considered to be mostly linear (Ohl & Ohl 1979; Schatten et al. 1978; Jiang et al. 2007). The toroidal field emerges to form active regions, hence the strength of toroidal field can be represented by the strength of solar cycle. The active regions usually have bipoles tilted against the east-west direction, and contributes net flux to the pole of opposite polarity, which is referred to as the B-L mechanism serving as the means of poloidal field generation from toroidal field. In the original iterative map of Durney (2000) and Charbonneau (2001), the newly generated poloidal

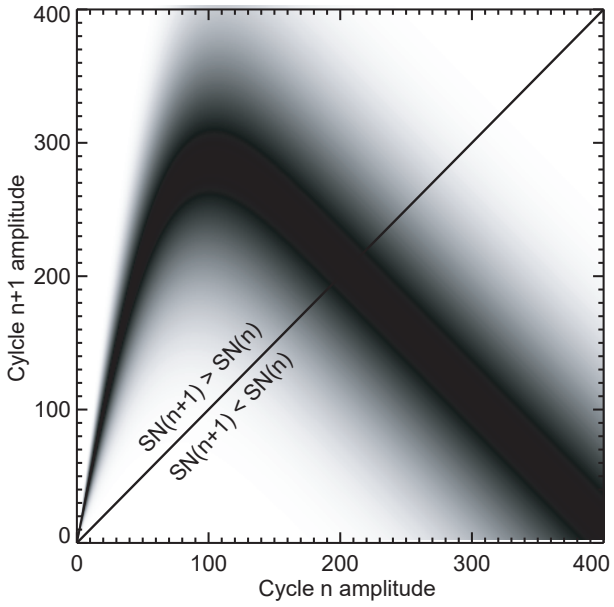

Figure 1. Diagram showing the relationship between cycle amplitude of cycles n+1 ($SN(n+1)$) and n ($SN(n)$) as described by Equation (1). The gray shaded region represents the distribution of probability density, with darker areas indicating higher likelihood. The diagonal line divides the plot into two regions: $SN(n+1) > SN(n)$ (upper-left) and $SN(n+1) < SN(n)$ (bottom-right).

field from toroidal field directly becomes the poloidal field at the beginning of the next cycle, but as we know that, in the B-L mechanism, the newly generated poloidal field should cancel out the old poloidal field first before building up that at the beginning of the next cycle. This is a major difference between our iterative map and earlier ones.

A significant advancement in understanding the solar cycle over the past decade is the quantification of intrinsic nonlinearity and stochasticity in the B-L mechanism for poloidal field generation, based on direct observations. The tilt angles of active regions during a stronger solar cycle tends to be smaller (Dasi-Espuig et al. 2010; Jiao et al. 2021), while the latitudes tends to be higher (Li et al. 2003; Solanki et al. 2008). These effects, referred to as tilt quenching and latitude quenching, respectively, limits the production of poloidal field from toroidal field, and serve as nonlinearity that confines cycle amplitudes in B-L dynamo (Jiang 2020; Karak 2020; Talafha et al. 2022). The stochasticity of B-L dynamo come from the turbulent convection affecting the rise and emergence of active region field (Weber et al. 2013), resulting in the large scatter of the latitude and tilt of active regions (Jiang et al. 2011, 2014). We use the quantification and parameterization of Jiang (2020), hereafter J20, to construct the iterative map.

With the linear poloidal to toroidal process and the nonlinear and stochastic toroidal to poloidal process, we finally create a recursion function of solar cycles, describing the relationship between the amplitude of cycle n+1, denoted as $SN(n+1)$, and the amplitude of cycle n, denoted as $SN(n)$. The recursion function is as follows

$$SN\left(n+1\right) = k_0 k_1 \mathbf{erf}\left(\frac{SN\left(n\right)}{quench}\right)\left(1 + stoch \times X\right) - SN\left(n\right), \tag{1}$$

in which k_0 is the correlation between axial dipole moment at cycle minimum and the next cycle's amplitude, k_1 and *quench* are parameters controlling nonlinearity, **erf** is the error function, X is a normally distributed random variable, and *stoch* is a parameter setting the standard deviation of stochasticity. The recursion function is illustrated in Figure 1.

The recursion function Equation (1) has 2 terms on the right-hand side. The first term is the poloidal field generation from toroidal field. Considering the property of error function, it first increases as the cycle amplitude $SN(n)$ increases, then saturates after $SN(n)$ is large enough. The parameter k_1 is the maximum amount of poloidal field that active regions can generate during a solar cycle in total, while *quench* controls how fast the poloidal field generation would saturate in terms of $SN(n)$. The random part $(1 + stoch \times X)$ is multiplicative to the error function, which indicates

that the actual scatter range should be larger when the poloidal field generation is larger. The first term of Equation (1) is subtracted by the second term, indicating that the generated poloidal field should cancel out the old poloidal field.

The parameters of nonlinearity and stochasticity has uncertainty because of observational limitations. Here, we adopt the parameters of J20 as the standard set of parameters, with maximum dipole moment k_1 being 6.94, *quench* being 75.85, and *stoch* being 0.17, in the following analysis. We also consider a considerable range of different parameters, evaluating the effect to the G-O rule.

The recursion function, along with an initial cycle amplitude, can be used to produce a large series of solar cycle amplitudes efficiently for the analysis of the G-O rule. We note that, the aforementioned quantification of nonlinearity and stochasticity is based on cycle amplitude (maximum value of the 13-month smoothed monthly sunspot number over a cycle in Sunspot Number Version 2). Hence, we use the current recursion function in the following analysis.

3. THE QUANTIFICATION OF THE G-O RULE IN THE ITERATIVE MAP

3.1. *Characteristics of Paired Cycles and Their Comparison with Observational Data*

Using the recursion function, i.e. Equation (1), we generate a large series of solar cycle amplitudes. We mainly focus on the cycle strength definition of the G-O rule, so we pair the cycles accordingly. We label the initial cycle as cycle 0, and then pair the cycles sequentially: 0-1, 2-3, 4-5, and so on. Each pair consists of an even cycle with the following odd cycle, which we refer to as G-O pairs. We then analyze the G-O rule in different forms and its variations based on these pairs in the following.

We first examine the proportion of pairs where the even cycle amplitude is larger than that of the following odd cycle. This is quantified by calculating the ratio of pairs with a larger even cycle to the total number of pairs, which we refer to as the E-to-A ratio. A summary of the definitions related to the G-O rule in the paper can be found in Table 1. We generate 1,000,000 cycles, pair them, and calculate the E-to-A ratio, which is found to be 0.4555 ± 0.0003, with the 1σ uncertainty being the standard error derived from 10 separate E-to-A ratio calculations. This result indicates that there are more pairs with the odd cycle larger than the even cycle. Interestingly, the initial cycle amplitude does not influence the ratio, whether the initial cycle is weak or strong. Furthermore, the starting index for pairing does not affect the outcome: if we label the first cycle as cycle 1, the cycle pairings are reversed, but the result remains the same. Regardless of the pairing method, the latter cycle in each pair consistently has a higher probability of being stronger than the former.

Having established that the latter cycles in the G-O pairs tend to be stronger, we now aim to quantify how much stronger they actually are. To do this, we analyze the difference between the two cycles in each pair, denoted as $\Delta SN = SN(2n+1) - SN(2n)$. This is similar to the analysis of Similä & Usoskin (2023). The probability density function (PDF) of ΔSN is shown in Figure 2, which indicates that ΔSN follows an asymmetric distribution. The mean of ΔSN is nearly 0, while the median is larger than 0, at 19. The standard deviation is large, at 157. This indicates that, in the half of the distribution where $\Delta SN > 0$, the population is larger, but the values of ΔSN are smaller. In contrast, for the half where $\Delta SN < 0$, the population is smaller, but the values are larger. Therefore, although the latter cycle is more likely to be larger than the former cycle, the expectation of the difference between the cycle strength within the G-O pairs is actually 0. Hence, there is no long-term trend of increasing cycle amplitude.

The aforementioned values of the E-to-A ratio and the PDF of ΔSN both have demonstrated the G-O rule holds. This rule likely arises from the nonlinearity and stochasticity inherent in the iterative map, as will be demonstrated in the following two subsections. We then examine the variations in the G-O rule. As reviewed in the introduction, some observations suggest that the G-O rule exhibits long term variations and reversal: some periods follow the G-O rule, while some periods follow a reversed G-O rule. To evaluate this, we define G-O blocks as continuous sequences of G-O pairs in which all pairs have larger even cycles or larger odd cycles, with opposite pairs before and after the block. We obtain the PDF of the block lengths based on the series of 1,000,000 cycles. As shown in Figures 3a and b, the length of G-O blocks follows an exponential distribution, which is a natural consequence of the stochastic process. Theoretically, if an event happens independently at a constant rate, the time interval between two such events will follow an exponential distribution. In our model, the probability of the pairs switching between even and odd is constant, meaning that the "reversal" of the G-O rule is not periodic, but rather random in our model. The block length PDF is compared with the results obtained from pairing cycles between 971 and 1900 reconstructed by Usoskin et al. (2021). For simplicity, we do not distinguish between normal cycles and grand minima cycles when determining the G-O blocks from the reconstructed cycles of Usoskin et al. (2021). Overall, the PDF follows the reconstructed

Table 1. List of concept definitions and roles in the G-O rule

Concept	Definition	Role in G-O rule
Even cycle	cycle with even number (e.g. 0,2,4,...)	the leading cycle in a cycle pair
Odd cycle	cycle with odd number (e.g. 1,3,5,...)	the following cycle in a cycle pair
G-O rule (cycle strength definition)	during a time range, more even cycles are weaker than their following odd cycles	
Reversed G-O rule (cycle strength definition)	during a time range, more even cycles are stronger than their following odd cycles	
E-to-A ratio	ratio of number of even-odd cycle pairs with larger even cycles to number of all even-odd cycle pairs	smaller than 0.5 indicates G-O rule while larger than 0.5 indicates reversed G-O rule
G-O block	a series of continuous cycle pairs with larger even (or odd) cycles	a logarithmic distribution would indicate the variation of G-O rule is stochastic
$SN(2n+1)-SN(2n)$	difference of cycle amplitude within an even-odd cycle pair	the asymmetricity and the median of its distribution imply G-O rule
$SN(n+1)-SN(n)$	difference of cycle amplitude between 2 arbitrary adjacent cycles	similar to above but without cycle pairing, its distribution suggests a general form of G-O rule
E-O correlation	Pearson's correlation between even cycles and following odd cycles	correlation definition of G-O rule suggests this correlation tends to be larger than the correlation below for a certain time range
O-E correlation	Pearson's correlation between odd cycles and following even cycles	

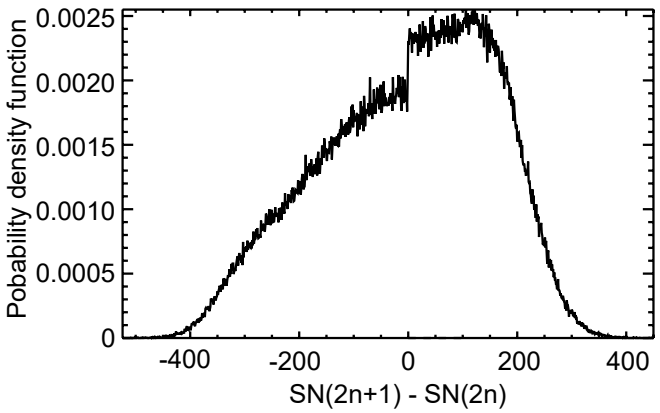

Figure 2. Probability density function (PDF) of the difference between the two solar cycles in each pair, derived from the 1,000,000 cycles generated using the recursion function, i.e., Equation (1).

cycle data. However, the relatively small number of observed solar cycles and their large uncertainty limit the ability of observational data to effectively constrain our model.

3.2. *The Impact of Nonlinearity and Stochasticity on the G-O Effect Behavior*

The key components of the iterative map are the B-L nonlinearity and stochasticity, so they should play a certain role in the G-O rule. In order to know how nonlinearity and stochasticity affects the G-O rule, we use different parameters, and observe how the E-to-A ratio is affected. This is also meaningful due to the fact that the parameters themselves are of uncertainty. We consider a $\pm 25\%$ variation of k_1, *quench*, and *stoch*, changing one parameter at a time while keeping others unchanged. In total, 6 cases are considered: $0.75 \times k_1$, $1.25 \times k_1$, $0.75 \times quench$, $1.25 \times quench$, $0.75 \times stoch$, and $1.25 \times stoch$. We also include an optimized set of parameters from our prequel paper, which is $k_1 = 6.94 \times 0.9, quench = 75.85 \times 1.5$, and $stoch = 0.17 \times 0.75$.

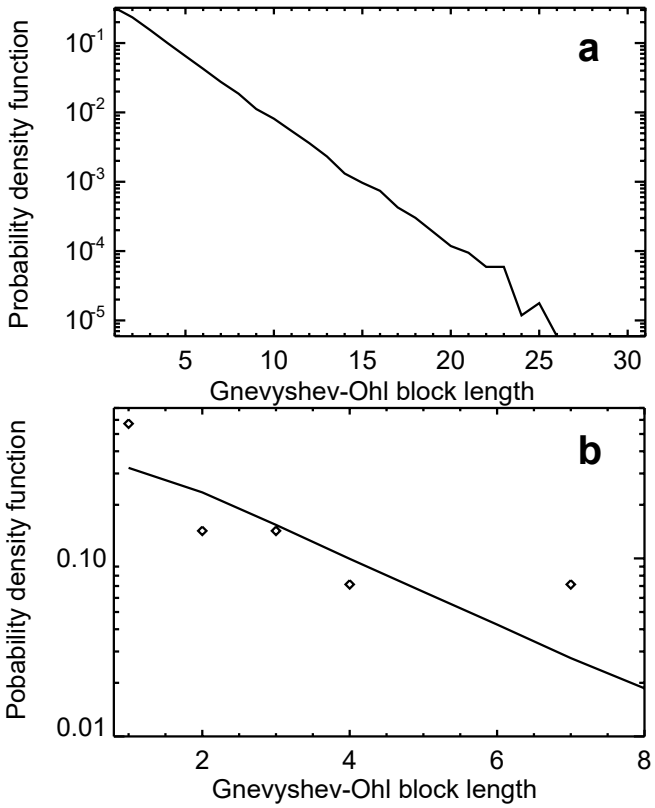

Figure 3. Statistical properties of the G-O pairs of cycles. **a,** The PDF of G-O block length with y axis in logarithmic scale. **b,** A zoom-in of **a** in order to compare with the results of Usoskin et al. (2021) including cycles during 971–1900, indicated by the diamond symbols.

We calculate different E-to-A ratios for the aforementioned 6 parameter sets. The uncertainty of each E-to-A ratio is again obtained from the standard error of 10 individual solar cycle series generated by the method. All produce a ratio below 0.5, confirming the validity of the G-O rule. Meanwhile, the E-to-A ratio reacts to parameter changes differently. Larger maximum dipole moment k_1 makes the ratio closer to 0.5, so the two types of pairs would be more similar, which means that the G-O rule is weaker. Larger *quench* or *stoch* decreases the ratio, enlarging the difference between the two types of pairs, indicating a stronger presence of G-O rule. The optimized set also produces a smaller E-to-A ratio compared to the standard set, which indicates that the G-O rule might be stronger in observations.

Usually, the G-O rule is explained by nonlinearity, which produces a strong cycle after a weak cycle and vice versa, thus forming a semi-regular pattern, while stochasticity is often considered to be destructive to semi-regular behavior. Our analysis actually shows that while the form of nonlinearity affects the G-O rule, the stochasticity is constructive to the G-O rule as well. The form and parameters of nonlinearity and stochasticity are both important to the G-O rule.

3.3. *The G-O Rule with a Limited Number of Solar Cycles*

The aforementioned results on the G-O rule are valid when the number of cycles is sufficiently large. However, real-world observations are based on a limited number of well-resolved solar cycles, which necessitates understanding how the G-O rule behaves with fewer cycles. Given that Similä & Usoskin (2023) analyzed a millennium of cycles, here we analyze 100 cycles, i.e., 50 G-O pairs. By analyzing a large set of such cycle series, we aim to derive the properties of the G-O rule when the number of cycles is limited.

We first examine whether there are more pairs in which the former cycle is larger than the latter cycle. There are a total of 100,000 series of cycles, and each series contains 100 cycles. Then, we obtain 100,000 E-to-A ratios, and produce the corresponding PDF in Figure 4a. The mean of the PDF is smaller than 0.5, but is not even of 1σ away from 0.5. This means that though there is a tendency of the limited cycles to follow the G-O rule, the cycles are not following the G-O rule in the statistically significant sense.

Table 2. E-to-A ratio of solar cycle series generated from different parameter sets of the iterative map

Parameter set	Ratio
standard set	0.4555 ± 0.0003
$0.75 \times k_1$	0.4371 ± 0.0002
$1.25 \times k_1$	0.4653 ± 0.0002
$0.75 \times quench$	0.4672 ± 0.0005
$1.25 \times quench$	0.4414 ± 0.0002
$0.75 \times stoch$	0.4754 ± 0.0002
$1.25 \times stoch$	0.4425 ± 0.0003
optimized set	0.4492 ± 0.0002

We also examine ΔSN under limited cycle numbers. As stated in Section 3.1, the median of ΔSN is larger than 0, which indicates that there are more cycles followed by a stronger cycle instead of weaker. Hence, here we produce the PDF of the median of ΔSN, shown in Figure 4b. Again, the median of ΔSN is larger than 0, but still not larger than the 1σ range, which implies that the G-O rule is not strictly followed.

We continue to examine the correlation definition of the G-O rule with a limited number of solar cycles. In the long run, the relationship between adjacent cycles will certainly follow Equation (1), regardless of even or odd, so we expect that the correlation definition is only applicable when cycle numbers are limited. We speculate that the initial amplitude of the limited cycle series is important. To test this, we let all 100,000 sets of 100 cycles to start at 2 amplitudes, $SN(0) = 81.2$, and $SN(0) = 285$, which are the weakest and strongest cycles since Cycle 1, correspondingly. Then, we observe the PDF of the E-O correlation and O-E correlation. The PDF of these correlations with $SN(0) = 81.2$ are plotted in Figures 5 a and b. As shown, both correlations are not quite likely to be significantly positive, or even somewhat positive at all. The E-O correlation seems to be slightly larger than O-E correlation for both set of parameters. We then show an example set of 100 cycles in Figure 5 c, in which the E-O correlation is larger than 0.9. As shown, in this example, most even-odd pairs (red) are located in the rising part of the recursion function, while odd-even pairs (blue) are not. The rising part of the recursion function is relatively more linear, so the correlation will be larger if the pairs of cycles fall into this range. For the case with $SN(0) = 285$, as shown in Figures 5 d and e, O-E correlation is more likely to be larger than E-O correlation, on the contrary, and the difference between the two correlation coefficients are larger under the optimized set of parameters. Another example in which the O-E correlation is larger than 0.9 is shown in Figure 5 f. This time, the odd-even (blue) pairs are more likely to fall into the linear region of the recursion function. This suggests that the correlation definition is dependent on the initial amplitude.

Our results show that, for limited cycles, the G-O rule by its cycle strength definition is only a trend and is not statistically significant even at 1σ significance. The behavior of solar cycles are more likely to form different G-O blocks, with some blocks having larger odd cycles, some having larger even cycles, and the total E-to-A ratio is not guaranteed to be either larger or smaller than 0.5. This favors the observational studies suggesting that there are variations of G-O rule, such as Mursula et al. (2001); Tlatov (2013); Zolotova & Ponyavin (2015). We note that the variations of G-O rule in our iterative map is random instead of systematic. As for the correlation definition of the G-O rule, it is in general a little more likely for E-O correlation to be larger than O-E correlation when the initial cycle amplitude is low, but still the correlation definition is not guaranteed under a limited number of cycles.

4. GENERAL UNDERSTANDING OF THE G-O RULE IN THE ITERATIVE MAP WITHOUT CYCLE PAIRING

In the previous section we have analyzed the different quantified forms of the G-O rule, which enable us to investigate the intrinsic origin of the G-O rule in this section. From Subsection 3.1, we know that the E-to-A ratio is unaffected by the method of pairing cycles. This implies that there is an inherent property of the cycles that does not require pairing them at all. In fact, the iterative map, which describes the relationship between cycle n and n+1, does not distinguish between even and odd cycles from the outset. As discussed in the first paper of the series, any solar cycle in the iterative map loses all its initial information after just a few iterations and becomes indistinguishable from all cycles in the statistical sense. This means that even and odd cycles are not distinguishable. This is true, as Figure 6a shows that even and odd cycles have the same PDF.

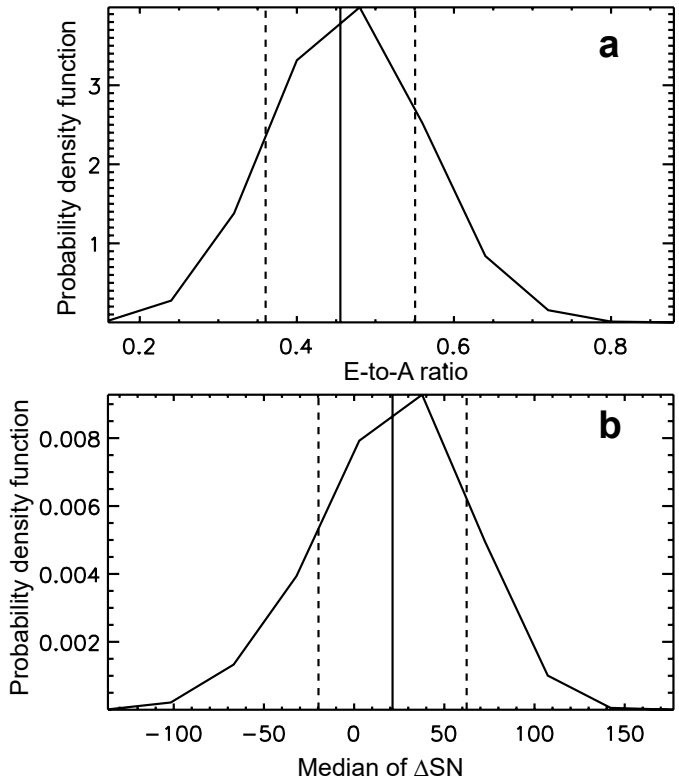

Figure 4. Statistical properties of the Gnevyshev-Ohl rule under 50 pairs of cycles. **a,** the PDF of E-to-A ratio, with the solid vertical line representing the mean and the dashed vertical lines representing 1σ range. **b,** the PDF of the median of ΔSN.

From this perspective, the G-O rule in the long run does not need pairing at all. For any 2 adjacent cycles, there is a larger probability for the latter cycle to be stronger than the former cycle. We evaluate this statement in the following. Let $p(x)$ be the PDF of x with x being $SN\,(n)$, and $q(y)$ be the PDF of y with y being $SN\,(n+1)$, then the G-O rule is to examine the following probability

$$P\,(y > x) = \int_{x=0}^{\infty} \int_{y=x}^{\infty} q\,(y)\,p\,(x)\,dydx. \tag{2}$$

The function $p(x)$ should be obtained by generating a large number of cycle amplitudes with Equation (1), and the result is presented in Figure 6a. The function $q(y)$ is a Gaussian distribution,

$$q\,(y) = \frac{1}{\sqrt{2\pi}\sigma_y} \exp\left(-\frac{(y- < y >)^2}{2\sigma_y^2}\right), \tag{3}$$

where $< y >= k_0 k_1 \mathbf{erf}\left(\frac{x}{quench}\right) - x$, and $\sigma_y = k_0 k_1 \mathbf{erf}\left(\frac{x}{quench}\right) \times stoch$. This comes from the recursion function. This probability can be calculated as long as we have the PDF $p(x)$. Using the PDF in Figure 6a, which is produced in the prequel to this paper, we have $P\,(y > x) = 0.546$. Then, the E-to-A ratio is 0.454, very close to the E-to-A ratio in Subsection 3.1.

Here we do not consider the ΔSN within pairs of cycles, but δSN of two arbitrary adjacent cycles. The PDF of δSN is actually $P\,(y = x + \delta SN)$, which is as follows,

$$P\,(y = x + \delta SN) = \int_{x=0}^{\infty} q\,(x + \delta SN)\,p\,(x)\,dydx. \tag{4}$$

The result of the integration of Equation (4) is presented in Figure 6b, which is identical to Figure 2, showing an asymmetric distribution on two sides and a discontinuity at 0. The discontinuity at 0 is a result of the property of the

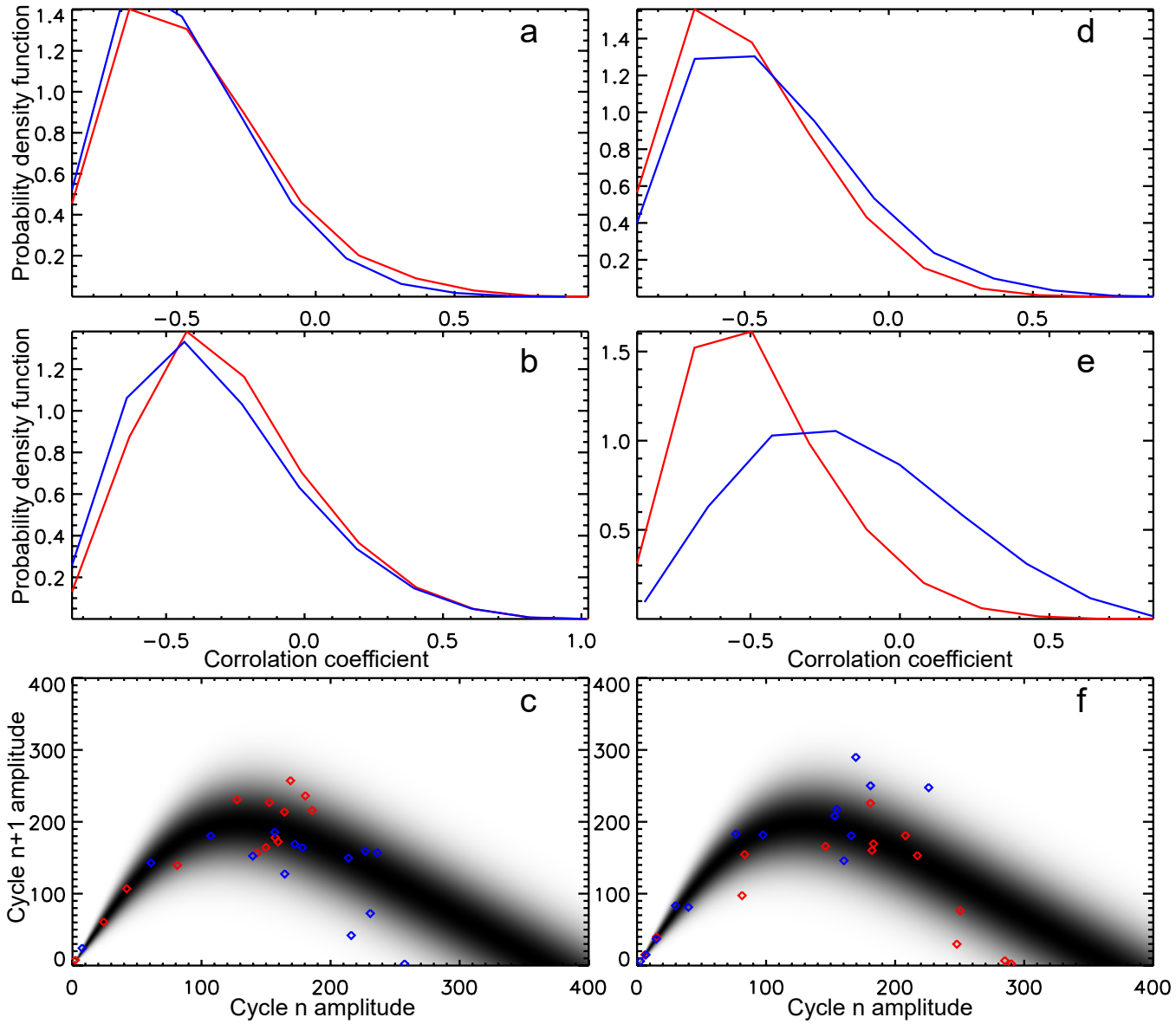

Figure 5. Statistical properties of 100,000 series of the Pearson correlation coefficient calculated for 50 pairs of even and odd cycles. Panels **a-c** corresponds to the case with initial cycle amplitude 81.2. **a,** the PDF of correlation coefficients under the standard set of parameters, in which the red curve indicates E-O correlation, while the blue curve indicates the O-E correlation. **b,** the same as **a**, but under the optimized set of parameters. **c,** relationship between cycle n and cycle n+1 amplitudes of one set of 50 pair of cycles in which E-O correlation is larger than 0.9, with red indicating n being even while blue indication n being odd, under the optimized set of parameters, and the shaded grey region indicates the recursion function with scatter range. Panels **d-f** are identical to panels **a-c**, respectively, except for the initial cycle amplitude being 285.

recursion function shown in Figure 1. The integration Equation (4) can be regarded as an integration of the recursion function along a line $y = x + \delta SN$, weighted by the PDF of cycle amplitude. As it is shown in Figure 1, when δSN is smaller than 0, such a line only covers the descending part of the recursion function. But when δSN becomes larger than 0, the ascending part of the recursion function is also included. Hence, the PDF of δSN is asymmetric and discontinuous.

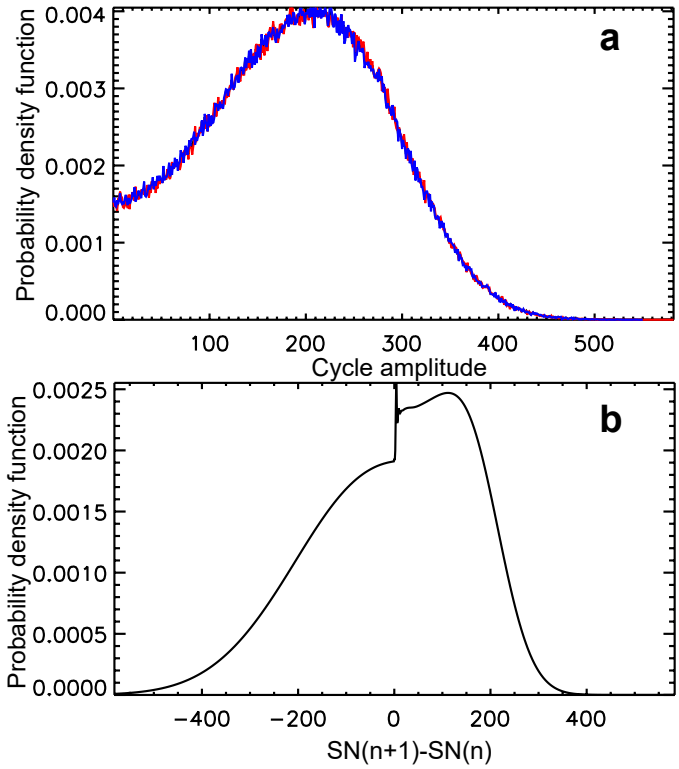

Figure 6. Probability density function of cycle amplitude (upper panel) and δSN (lower panel). The curve in the upper panel is actually composed of 3 overlaid curves, which are a black curve referring to all cycle amplitude, a red curve indicating even cycle amplitude, and a blue curve showing odd cycle amplitude.

Surely enough, the long term G-O rule of the iterative map is a direct result of the nonlinearity and stochasticity in the B-L mechanism. The heterogenity of stochasticity and the form of nonlinearity cause that weaker cycles are more likely to have following stronger cycles. That is, a weak cycle is more certain to be followed by a stronger cycle, while a strong cycle is less certain to be followed by a weaker cycle. This, along with the PDF of cycle amplitudes, together generates the long term G-O rule without the definitions of cycle pairs. This also explain the reason why increasing stochasticity is constructive to the G-O rule, as the heterogenity is also increased. We note that, "cycles are more likely to be followed by a larger cycle" does not result in unbounded growth of cycle strength. The cycles in this statement is an arbitrary cycle among the PDF of cycles. For a definite cycle, whether the next cycle is probably stronger or weaker is solely determined by Equation (1). Statistically, while δSN is more likely to be positive, the absolute values of positive δSN are smaller than negative, so the cycle amplitude is not unbounded.

When the total cycle number is limited, the G-O rule under the cycle strength definition is only a trend instead of a statistical significant result. The correlation definition of the G-O rule is possible to occur but still not guaranteed. Consider a weak starting cycle $SN(0)$, it is possible that a certain number of cycles after this weak cycle follow the weak-strong pattern of the G-O rule. Then, all even cycles are relatively weaker to the odd cycles. According to the recursion function shown in Figure 1, weaker cycles fall into the ascending part of the function which is closer to linear relationship and has less scatter, while stronger cycles fall into the nonlinear, with more scatter, descending part. On the other hand, when the initial amplitude is strong, the cycles are likely to follow the strong-weak pattern, then the odd cycles are more likely to fall into the linear part of the recursion function. This provides a possible explanation that why the E-O correlation may be larger than O-E correlation in our model.

5. DISCUSSION AND CONCLUSIONS

In this article, we have analyzed the G-O rule in the iterative map based on the observationally constrained B-L nonlinearity and stochasticity, obtained in the prequel to this paper. Within the framework of B-L dynamo, there is

larger possibility for an arbitrary cycle to have a stronger following cycle instead of a weaker one. This property results in the G-O rule in the long run when the cycles are paired up, but pairing is actually not needed. In short periods lasting a millennium or even shorter, the solar cycle only shows a trend to strictly follow G-O rule but not of statistical significance. The cycles are more likely to occasionally convert from the G-O rule to the "reversed" G-O rule and vice versa at random instead of having a notable preference over either case, which agrees with the observational studies that shows possible variations of the G-O rule.

In the iterative map that generates the G-O rule, one cycle solely determines the next, and there is no longer-than-1-cycle memory. From this perspective, it is not necessary to consider the Hale 22-year cycle as the fundamental component of solar cycle evolution in order to explain the G-O rule, nor is other long-term memory or fossil field needed. Still, we do not completely rule out the possibility of other explanations.

The G-O rule in the iterative map is a direct product of the nonlinearity and stochasticity intrinsic in the B-L dynamo. The nonlinearity and stochasticity produces a PDF of cycle amplitudes, and this PDF is integrated along with the recursion function of the cycle amplitude to produce the G-O rule. Therefore, our results again emphasis the importance of better understanding of the nonlinearity and stochasticity of solar cycle evolution, including both their form and their parameters.

Future advance in the solar cycle recursion relation under the framework of B-L dynamo will be able to provide better explanation to the G-O rule. Such advance requires more accurately observed solar cycles and better understanding of the B-L mechanisms. In the foreseeable future, we consider that it is unlikely for the number of clearly resolved cycle to be sufficient to determine the E-to-A ratio with statistical significance. The G-O rule will be a trend not a solid rule under the framework of B-L dynamo, therefore, in the study of solar dynamo, the G-O rule on its own cannot be used as a strict observational constraint on solar dynamo modeling. The G-O rule cannot be used to predict solar cycle totally on its own either. The understanding and utilization of the G-O rule should be combined with other properties of solar cycle evolution.

This research was supported by the National Natural Science Foundation of China through Grant Nos. 12425305, 12350004, 12173005, 12373111, & 12273061, the National Key R&D Program of China through Grant Nos. 2022YFF0503800, 2019YFA0405000, 2021YFA1600500, & 2022YFF0503000; the Strategic Priority Program of Chinese Academy of Sciences through Grant Nos. XDB41000000 & XDB0560000; and the Key Research Program of Frontier Sciences of CAS through Grant No. ZDBS-LY-SLH013.

REFERENCES

Babcock, H. W. 1961, Astrophysical Journal, 133, 572, doi: 10.1086/147060

Charbonneau, P. 2001, Solar Physics, 199, 385, doi: 10.1023/A:1010387509792

—. 2005, Living Reviews in Solar Physics, 2, 2, doi: 10.12942/lrsp-2005-2

—. 2020, Living Reviews in Solar Physics, 17, 4, doi: 10.1007/s41116-020-00025-6

Charbonneau, P., St-Jean, C., & Zacharias, P. 2005, Astrophysical Journal, 619, 613, doi: 10.1086/426385

Dasi-Espuig, M., Solanki, S. K., Krivova, N. A., Cameron, R., & Peñuela, T. 2010, Astronomy and Astrophysics, 518, A7, doi: 10.1051/0004-6361/201014301

Durney, B. R. 2000, Solar Physics, 196, 421, doi: 10.1023/A:1005285315323

Gnevyshev, M. N., & Ohl, A. I. 1948, Astronomicheskii Zhurnal, 25, 18

Hale, G. E., Ellerman, F., Nicholson, S. B., & Joy, A. H. 1919, Astrophysical Journal, 49, 153, doi: 10.1086/142452

Hathaway, D. H. 2015, Living Reviews in Solar Physics, 12, 4, doi: 10.1007/lrsp-2015-4

Javaraiah, J. 2012, SoPh, 281, 827, doi: 10.1007/s11207-012-0106-6

Jiang, J. 2020, Astrophysical Journal, 900, 19, doi: 10.3847/1538-4357/abaa4b

Jiang, J., Cameron, R. H., Schmitt, D., & Işık, E. 2013, A&A, 553, A128, doi: 10.1051/0004-6361/201321145

Jiang, J., Cameron, R. H., Schmitt, D., & Schüssler, M. 2011, A&A, 528, A82, doi: 10.1051/0004-6361/201016167

Jiang, J., Cameron, R. H., & Schüssler, M. 2014, Astrophysical Journal, 791, 5, doi: 10.1088/0004-637X/791/1/5

Jiang, J., Chatterjee, P., & Choudhuri, A. R. 2007, Monthly Notices of the Royal Astronomical Society, 381, 1527, doi: 10.1111/j.1365-2966.2007.12267.x

Jiao, Q., Jiang, J., & Wang, Z.-F. 2021, Astronomy and Astrophysics, 653, A27, doi: 10.1051/0004-6361/202141215

Karak, B. B. 2020, ApJL, 901, L35, doi: 10.3847/2041-8213/abb93f

Leighton, R. B. 1969, Astrophysical Journal, 156, 1, doi: 10.1086/149943

Li, K. J., Wang, J. X., Zhan, L. S., et al. 2003, Solar Physics, 215, 99, doi: 10.1023/A:1024814505979

May, R. M. 1976, Nature, 261, 459, doi: 10.1038/261459a0

Mursula, K., Usoskin, I. G., & Kovaltsov, G. A. 2001, SoPh, 198, 51, doi: 10.1023/A:1005218414790

Nagovitsyn, Y. A., Osipova, A. A., & Ivanov, V. G. 2024, Astronomy Reports, 68, 89, doi: 10.1134/S1063772924700069

Ohl, A. I., & Ohl, G. I. 1979, in NOAA Solar-Terrestrial Predictions Proceedings. Volume 2., ed. R. F. Donnelly, Vol. 2, 258–263

Parker, E. N. 1955, Astrophysical Journal, 122, 293, doi: 10.1086/146087

Schatten, K. H., Scherrer, P. H., Svalgaard, L., & Wilcox, J. M. 1978, Geophys. Res. Lett., 5, 411, doi: 10.1029/GL005i005p00411

Similä, M., & Usoskin, I. 2023, in IAU Symposium, Vol. 372, The Era of Multi-Messenger Solar Physics, ed. G. Cauzzi & A. Tritschler, 70–75, doi: 10.1017/S1743921323000236

Solanki, S. K., Wenzler, T., & Schmitt, D. 2008, Astronomy and Astrophysics, 483, 623, doi: 10.1051/0004-6361:20054282

Talafha, M., Nagy, M., Lemerle, A., & Petrovay, K. 2022, Astronomy and Astrophysics, 660, A92, doi: 10.1051/0004-6361/202142572

Tlatov, A. G. 2013, ApJL, 772, L30, doi: 10.1088/2041-8205/772/2/L30

Turner, H. H. 1925, MNRAS, 85, 467, doi: 10.1093/mnras/85.5.467

Usoskin, I. G., Mursula, K., Arlt, R., & Kovaltsov, G. A. 2009, ApJL, 700, L154, doi: 10.1088/0004-637X/700/2/L154

Usoskin, I. G., Mursula, K., & Kovaltsov, G. A. 2001, A&A, 370, L31, doi: 10.1051/0004-6361:20010319

Usoskin, I. G., Solanki, S. K., Krivova, N. A., et al. 2021, Astronomy and Astrophysics, 649, A141, doi: 10.1051/0004-6361/202140711

Weber, M. A., Fan, Y., & Miesch, M. S. 2013, SoPh, 287, 239, doi: 10.1007/s11207-012-0093-7

Zolotova, N. V., & Ponyavin, D. I. 2015, Geomagnetism and Aeronomy, 55, 902, doi: 10.1134/S0016793215070300